INVESTIGACIÓN E INNOVACIÓN EN INGENIERÍAS

Exploring the impact of 3D printing parameters on mechanical properties of ABS and PLA materials through machine learning analysis

Exploración del impacto de los parámetros de impresión 3D en las propiedades mecánicas de los materiales ABS y PLA mediante análisis de aprendizaje automático

Vladimir Cudris Guerrero

Institución Universitaria de Barranquilla

OPEN ACCESS

Recibido: 28/11/2023
Aceptado: 12/01/2024
Publicado: 28/02/2024

Correspondencia de autores:
vcudris@unibarranquilla.edu.co

Abstract

Objective: This research presents a comprehensive experimental study on the effect of temperature, material and process parameters related to tensile strength response in 3D printing manufacturing process with ABS material. **Methodology or method:** A Hyper Latin Square design was chosen for the experimental points' distribution. Thirteen parameters with multiple levels are considered LAYERHEIGHT, WALLTHICKNESS, TOPBOTTOMTHICKNESS, TOPBOTTOMLINEDIRECTION1, TOPBOTTOMLINEDIRECTION2, INFILLDENSITY, INFILLLINEDIRECTION1, INFILLLINEDIRECTION2, PRINTSPEED, EXTRUSIONTEMP, BEDTEMP, WORKSPACETEMP and POSITION. **Results:** Type IV tensile specimens are fabricated and tested with a universal testing machine. Maximum stress is measured, evaluated and analyzed in three different building positions. Machine learning algorithm with Orange Data mining software are used to study underlying relations between factors and response. Experimental results indicate that INFILLDENSITY, TOPBOTTOMTHICKNESS and INFILLLINEDIRECTION1 has a strong positive correlation with mechanic properties for ABS and PLA. Meanwhile, TOPBOT-TOMLINEDIRECTION1, WORKSPACETEMPERATURE and PRINTSPEED has a negative correlation with tensile strength. Position 1 and 3 with line depositions parallel to Y axis produce the higher tensile strength response. **Conclusions:** Findings imply that machine algorithms can be used to study multiple parameters at a time.

Keywords: ABS, PLA, fused deposition modelling, print 3D, parameters, machine learning, tensile strength.

Resumen

Objetivo: Esta investigación presenta un estudio experimental exhaustivo sobre el efecto de la temperatura, el material y los parámetros del proceso relacionados con la respuesta de resistencia a la tracción en el proceso de fabricación de impresión 3D con material ABS. **Metodología o método:** Se eligió un diseño hipercuadrado latino para la distribución de los puntos experimentales. Se consideraron trece parámetros con múltiples niveles: LAYERHEIGHT, WALLTHICKNESS, TOPBOTTOMTHICKNESS, TOPBOTTOM- LINEDIRECTION1, TOPBOT-TOMLINEDIRECTION2, INFILLDENSITY, INFILLLINEDIRECTION1, INFILLLINEDIRECTION2, PRINTSPEED, EXTRUSIONTEMP, BEDTEMP, WORKSPACETEMP y POSITION. **Resultados:** Se fabrican probetas de tracción de tipo IV y se ensayan con una máquina universal de ensayos. Para estudiar las relaciones subyacentes entre los factores y la respuesta se utiliza un algoritmo de aprendizaje automático con el software de minería de datos Orange. Los resultados experimentales indican que INFILLDENSITY, TOPBOTOMTOMTHICKNESS e INFILLLINEDIRECTION1 tienen una fuerte correlación positiva con las propiedades mecánicas del ABS y el PLA. Mientras tanto, TOPBOT- TOMLINEDIRECTION1, WORKSPACETEMPERATURE y PRINTSPEED tienen una correlación negativa con la resistencia a la tracción. Las posiciones 1 y 3 con deposiciones de líneas paralelas al eje Y producen la respuesta de mayor resistencia a la tracción. **Conclusiones:** Los resultados indican que los algoritmos de máquina pueden utilizarse para estudiar varios parámetros a la vez.

Palabras clave: ABS, PLA, modelado por deposición fundida, impresión 3D, parámetros, aprendizaje automático, resistencia a la tracción.

Como citar (IEEE): V. Cudris Guerrero. "Exploring the impact of 3D printing parameters on mechanical properties of ABS and PLA materials through machine learning analysis". Investigación e Innovación en Ingenierías, vol. 12, n°1, 31-29, 2024. DOI: https://doi.org/10.17081/invinno.12.1.6803

Introduction

3D printing [1], a revolutionary additive manufacturing process, has ushered in a new era of manufacturing capabilities by allowing the creation of intricate three-dimensional objects with unparalleled precision and adaptability. The pivotal role of 3D printing parameters in shaping the mechanical properties of printed objects cannot be understated. In this article, we embark on an exploration of the intricate relationship between various printing parameters and the resultant mechanical properties, focusing on two ubiquitous materials in 3D printing: Acrylonitrile Butadiene Styrene (ABS) and Poly lactic Acid (PLA). Moreover, we introduce a novel dimension to this investigation by incorporating machine learning techniques to comprehensively analyze and predict the intricate interplay between these parameters and mechanical outcomes. The dominant approach within the domain of Fused Deposition Modeling (FDM) is embodied by 3D printing, necessitating meticulous control over an array of process parameters. These encompass a suite of process-related variables, including deposition angle, layer height, fabrication orientation, deposition width, print speed, fill density, air gaps, fill patterns, and extrusion temperature. In tandem, the orchestration of workspace parameters, comprising bed temperature, chamber temperature, humidity levels, and nozzle diameter, assumes a pivotal role. Additionally, the manipulation of material parameters, encompassing material composition, coloration, and filament diameter, serves as an indispensable facet requiring exacting calibration to attain the desired outcomes. [2].

Figure 1. Schematic representation of Print 3D basic machine. a)Filament, b)Extruder, c)Model, d)Supports, e)Bed, f)Work space

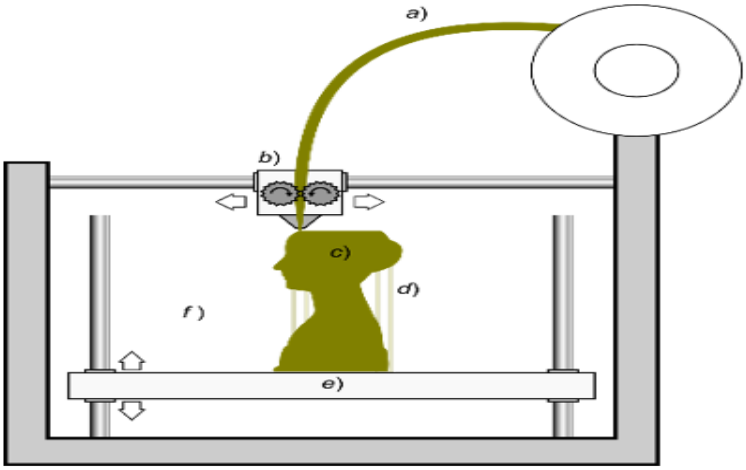

Source: PNGWING.

In the context of 3D printing, thorough investigations have been conducted to explore the parameters and their consequential influence on the properties and behavior of the fabricated part. A substantial portion of this research is focused on the analysis of mechanical properties, particularly encompassing attributes such as tensile resistance, compressive strength, bending behavior, torsional characteristics, and the capacity to absorb impact energy. [1, 2, 3].

The investigation of tensile stress within the context of 3D printing has received substantial attention from various researchers. This mechanical property stands as a cornerstone for components manufactured through this method, as their intended applications often demand a notable capacity to withstand such stress. These studies have embraced diverse statistical methodologies, including factorial design, as evidenced in works such as [4, 5, 6, 7, 8, 9]. Additionally, the utilization of response surface methodology is apparent in studies such as [10, 11, 12, 13, 14], while the Taguchi approach has been implemented in investigations like [15, 16, 17, 18, 19]. Furthermore, the application of machine learning algorithms has also come to the fore, as evident from references like [20] and [21].

3D print Material

Within the scope of this scientific inquiry, our attention is directed towards the comprehensive analysis of two prominent materials: Acrylonitrile Butadiene Styrene (ABS) and Poly lactic Acid (PLA). These materials have been chosen based on their widespread utilization and significance in the domain of additive manufacturing and 3D printing. Their distinctive

material properties, coupled with their versatile applicability, render them prime subjects for a meticulous investigation into their mechanical attributes and behaviors. Materials are from eSUN brand, red color, with the properties and printing parameters recommended in Table 1.

Table 1. Filament Properties Comparison - ABS vs. PLA

3D PRINTING FILAMENT	ABS	PLA
Density (g/cm3)	1.04	1.23
Heat Distortion Temp (°C, 0.45MPa)	78	53
Melt Flow Index (g/10min)	12 (220 °C/10kg)	5 (190 °C/2.16kg)
Tensile Strength (MPa)	43	60
Elongation at Break (%)	22	20
Flexural Strength (MPa)	66	74
Flexural Modulus (MPa)	1177	1973
IZOD Impact Strength (kJ/m2)	29	6
RECOMMENDED PRINTING PARAMETERS		
Extruder Temperature (°C)	230 – 270	210 – 230
Recommended temperature	240	215
Bed temperature (°C)	95 – 110	45 – 60
Fan Speed	0%	100%
Printing Speed	40 – 100 mm/s	40 – 100 mm/s
Heated Bed	Required	Optional

Source: eSUN

3D printing machine

The printer used for the fabrication of the test specimens is a INTAMSYS FUNMAT HT (Figure 2) with a build volume of 260 x 260 x 260 mm with 50-micron high-resolution industrial quality 3D printing. The thermal system design of this 3D printer includes a 90 °C constant temperature chamber, 160 °C heated build plate and 450 °C high-temperature extruder with an all-metal hot end.

Figure 2. INTAMSYS 3d printer From INTAMSYS)

Source: INTAMSYS.

Printing process parameters

Ten process parameters are included for the research:

- Temperature parameters
  - Extrusion temperature (EXTRUSIONTEMP)
  - Platform temperature (BEDTEMP)
  - Workspace temperature (WORKSPACETEMP)
- Machine parameters
  - Print velocity (PRINTSPEED)
- Material deposition parameters
  - Layer height (LAYERHEIGHT)
  - Wall thickness (WALLTHICKNESS)
  - Top and bottom layer thickness (TOPBOTTOMTHICKNESS)
  - Top and bottom layer line directions (TOPBOTTOMLINEDIRECTION)
  - Infill density (INFILLDENSITY)
  - Infill line direction (INFILLLINEDIRECTION)
  - Build Orientation (POSITION)

Factor parameter levels

The chosen experimental design for assessing the impact of process factors on the output was a Latin Hypercube Sampling (LHS). This design was selected due to its capability to provide a more uniform distribution of random sample experimental points [22]. The level ranges were determined based on prior research and are presented in Table 2.

Table 2. Factors a range for the experimental points sample design

FACTOR	LEVEL INTERVAL
(LH) LAYERHEIGHT (mm)	0.1, 0.2, 0.3
(WT) WALLTHICKNESS	0.6, 0.8, 1
(TBT) TOPBOTTOMTHICKNESS (mm)	0.4, 0.8, 1
(TBLD1) TOPBOTTOMLINEDIRECTION1 (°)	0, 180
(TBLD2) TOPBOTTOMLINEDIRECTION2 (°)	0, 180
(ID) INFILLDENSITY (%)	20, 50, 80, 100
(ILD1) INFILLLINEDIRECTION1 (°)	0, 180
(ILD2) INFILLLINEDIRECTION2 (°)	0, 180
(PS) PRINTSPEED (mm/sec)	40, 60, 80
(ET) EXTRUSIONTEMP (°C)	220, 260
(BT) BEDTEMP (°C)	80, 100
(WST) WORKSPACETEMP (°C)	30, 60
(POS) POSITION	P1, P2, P3

Source: Own elaboration.

Applying the LHS for the distribution of the experimental points, a set of data is obtained as shown in Table 3.

Printing process

The SolidWorks models were saved in the stl format and underwent preprocessing using Ultimaker Cura slicer software. Test specimens were printed in three distinct positions, each sharing identical parameters, to facilitate a comparison of the impact of the same experimental point across these varied building positions. Refer to Figure 3 for a visual representation.

Tensile testing

Testing specimen: The tension test specimens adhere to ASTM D638 Type IV standards [23]. These specimens were designed using SolidWorks software, maintaining dimensions as illustrated in Figure 4.

Table 3. Experimental points generated with LHS

RUN	LH	WT	TBT	TBLD1	TBLD2	ID	ILD1	ILD2	WST	ET	BT	PS	POS
1	0.21	0.78	0.87	140	80	64.44	60	20	46.67	220.00	100.00	44.44	P1
2	0.21	0.78	0.87	140	80	64.44	60	20	46.67	220.00	100.00	44.44	P2
3	0.10	0.96	0.80	80	40	91.11	180	160	36.67	260.00	91.11	62.22	P1
4	0.10	0.96	0.80	80	40	91.11	180	160	36.67	260.00	91.11	62.22	P2
5	0.10	0.96	0.80	80	40	91.11	180	160	36.67	260.00	91.11	62.22	P3
6	0.30	0.82	0.73	0	0	28.89	20	40	33.33	224.44	97.78	66.67	P1
7	0.30	0.82	0.73	0	0	28.89	20	40	33.33	224.44	97.78	66.67	P2
8	0.30	0.82	0.73	0	0	28.89	20	40	33.33	224.44	97.78	66.67	P3
9	0.19	1.00	1.00	60	120	55.56	120	0	30.00	255.56	93.33	40.00	P1
10	0.19	1.00	1.00	60	120	55.56	120	0	30.00	255.56	93.33	40.00	P2
11	0.19	1.00	1.00	60	120	55.56	120	0	30.00	255.56	93.33	40.00	P3
12	0.12	0.60	0.53	160	140	46.67	140	100	50.00	228.89	95.56	57.78	P1
13	0.12	0.60	0.53	160	140	46.67	140	100	50.00	228.89	95.56	57.78	P2
14	0.12	0.60	0.53	160	140	46.67	140	100	50.00	228.89	95.56	57.78	P3
15	0.28	0.64	0.93	20	180	100.00	160	120	40.00	233.33	86.67	48.89	P1
16	0.28	0.64	0.93	20	180	100.00	160	120	40.00	233.33	86.67	48.89	P2
17	0.28	0.64	0.93	20	180	100.00	160	120	40.00	233.33	86.67	48.89	P3
18	0.14	0.69	0.40	100	20	37.78	0	80	56.67	242.22	84.44	75.56	P1
19	0.14	0.69	0.40	100	20	37.78	0	80	56.67	242.22	84.44	75.56	P2
20	0.14	0.69	0.40	100	20	37.78	0	80	56.67	242.22	84.44	75.56	P3
21	0.17	0.87	0.47	40	160	82.22	100	140	60.00	246.67	82.22	80.00	P1
22	0.17	0.87	0.47	40	160	82.22	100	140	60.00	246.67	82.22	80.00	P2
23	0.17	0.87	0.47	40	160	82.22	100	140	60.00	246.67	82.22	80.00	P3
24	0.23	0.91	0.60	120	100	20.00	80	180	43.33	251.11	88.89	53.33	P1
25	0.23	0.91	0.60	120	100	20.00	80	180	43.33	251.11	88.89	53.33	P2
26	0.23	0.91	0.60	120	100	20.00	80	180	43.33	251.11	88.89	53.33	P3
27	0.26	0.73	0.67	180	60	73.33	40	60	53.33	237.78	80.00	71.11	P1

RUN	LH	WT	TBT	TBLD1	TBLD2	ID	ILD1	ILD2	WST	ET	BT	PS	POS
28	0.26	0.73	0.67	180	60	73.33	40	60	53.33	237.78	80.00	71.11	P2
29	0.26	0.73	0.67	180	60	73.33	40	60	53.33	237.78	80.00	71.11	P3

Source: Own elaboration.

Figure 3. The three positions of the testing specimens

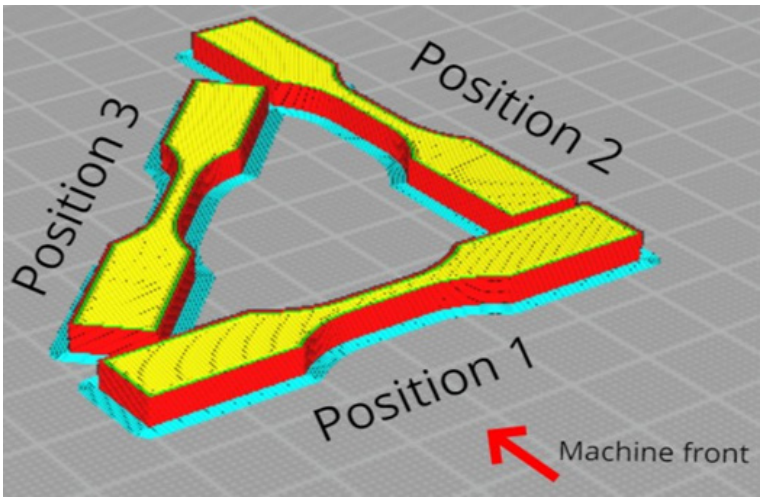

Source: Own elaboration.

The Universal Testing Machine used in this study is the 50 kN Armsfield model. The testing velocity was maintained at 1 mm. Following each test, the stress-strain curves and resultant data were documented within the machine's software. Parameters such as yield, ultimate and fracture stress, as well as the maximum load, were extracted from these graphical representations. Furthermore, the calculation of Young's modulus was derived from the gradient of the stress-strain curves.

Figure 4. ASTM D638 Type IV Tension test specimen with dimensions in mm

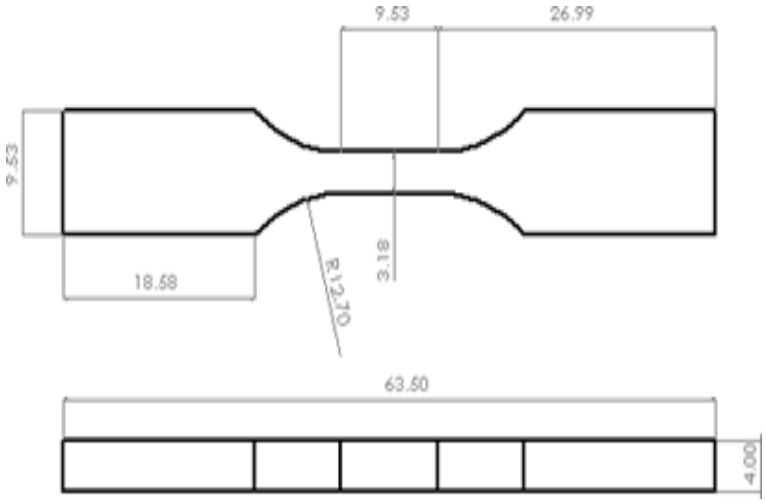

Source: Own elaboration.

Machine learning processing

In the field of machine learning analysis, the employment of a visual data mining tool played a crucial role. For this specific task, we opted for Orange Data Mining [24], a software application designed for data mining and predictive analytics. Created at the Faculty of Informatics at the University of Ljubljana, Orange comprises a collection of components built in C++. These components encompass various data mining algorithms, data preprocessing capabilities, and tools for graphical representation, as illustrated in Figure 5. One remarkable advantage of Orange is its accessibility; exploring data using this tool doesn't require programming expertise or an extensive understanding of mathematics.

Figure 5. Orange workflow example

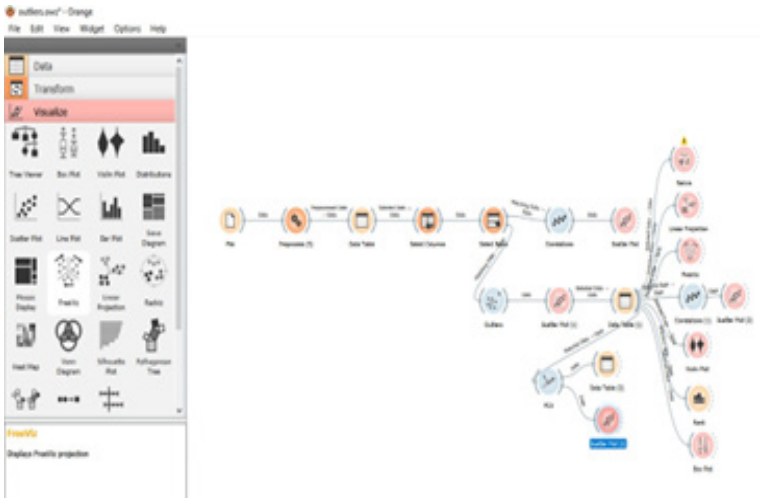

Source: Own elaboration.

Results

Tensile test results

Table 4 shows calculated results for the tension tests.

Correlation results

For the correlation's analysis, Pearson method was computed [25]. Results in Table 5 and Table 6 shows that positive and negative correlation exist between factors and the maximum stress, break stress and Young's Module.

Table 4. Results measure from tensile tests

RO	MATERIAL	MAX LOAD (N)	BREAK LOAD (N)	MAX STRESS	DEF MAX	BREAK STRESS	DEF BREAK	E (MPa)
1 1	ABS	255	200	21.15	0.214	16.587	0.258	159.11
1 2	ABS	267	217	22.14	0.614	19.41	0.648	147.28
2 1	ABS	435	416	36.08	0.47	34.5	0.488	258.71
2 2	ABS	255	231	21.15	0.256	19.16	0.28	149.55
2 3	ABS	323	292	26.79	0.442	24.22	0.47	167.3
3 1	ABS	128	112	10.62	0.172	9.29	0.17	90.23

RO	MATERIAL	MAX LOAD (N)	BREAK LOAD (N)	MAX STRESS	DEF MAX	BREAK STRESS	DEF BREAK	E (MPa)
3 2	ABS	179	150	14.84	0.204	12.44	0.216	101.26
3 3	ABS	188	166	15.6	0.28	13.77	0.28	83.23
4 1	ABS	232	173	19.24	0.204	15.67	0.234	112.79
4 2	ABS	248	186	20.57	0.294	15.43	0.37	114.14
4 3	ABS	212	189	17.58	0.252	15.67	0.268	151.02
5 1	ABS	138	123	11.4	0.184	10.2	0.189	89.5
5 2	ABS	123	121	10.2	0.238	10.03	0.24	70.11
5 3	ABS	94	82	7.79	0.21	6.8	0.218	98.1
6 1	ABS	300	236	24.88	0.2	19.57	0.254	191.04
6 2	ABS	318	262	26.37	0.178	21.73	0.254	218.87
6 3	ABS	289	267	24	0.134	22.14	0.16	223.82
7 1	ABS	153	136	12.69	0.256	11.28	0.266	107.57
7 2	ABS	157	137	13.02	0.234	11.36	0.254	106.57
7 3	ABS	142	97	11.77	0.298	8.04	0.374	84.71
8 1	ABS	335	322	27.78	0.468	26.7	0.476	224.92
8 2	ABS	210	1.58	14.42	0.214	13.1	0.264	145.04
8 3	ABS	192	168	15.92	0.144	13.93	0.158	148.13
9 1	ABS	178	92	14.76	0.23	7.63	0.314	109.17
9 2	ABS	160	135	13.27	0.284	11.2	0.298	75.3
9 3	ABS	153	120	12.69	0.284	9.95	0.322	70.04
10 1	ABS	206	174	17.08	0.218	14.43	0.254	104.11
10 2	ABS	176	128	14.6	0.2	10.62	0.234	131.54
10 3	ABS	185	172	15.34	0.174	14.26	0.198	137.87
1 1	PLA	389	149	32.26	0.594	12.36	0.798	297.67
1 2	PLA	472	430	39.15	0.62	35.66	0.644	257.6
1 3	PLA	493	419	40.89	0.508	34.75	0.574	313.81
2 1	PLA	421	378	34.92	0.56	33.01	0.634	159.84
2 2	PLA	318	238	26.37	0.33	19.74	0.38	250.53
2 3	PLA	494	467	40.97	0.63	38.73	0.668	157.8
3 1	PLA	295	218	24.47	0.63	18.08	0.692	111.23
3 2	PLA	422	392	35	0.61	31.51	0.652	134.83
3 3	PLA	363	320	30.11	0.56	26.54	0.622	183.15
4 1	PLA	422	363	35	0.478	30.12	0.532	325.94
4 2	PLA	404	396	33.51	0.542	32.84	0.55	130.14
4 3	PLA	482.7	442	40.14	0.504	36.66	0.556	181.84
5 1	PLA	377.5	370	31.29	0.522	30.69	0.536	158.22
5 3	PLA	209	194	17.29	0.56	16.09	0.602	139.26
6 1	PLA	629	477	52.17	0.506	39.56	0.658	284.12
6 2	PLA	393	299	32.59	0.312	24.71	0.45	265.26

RO	MATERIAL	MAX LOAD (N)	BREAK LOAD (N)	MAX STRESS	DEF MAX	BREAK STRESS	DEF BREAK	E (MPa)
6 3	PLA	566	364	46.94	0.476	30.19	0.764	151.94
7 1	PLA	376	357	31.18	0.588	29.608	0.638	152.21
7 2	PLA	300	253	24.88	0.542	20.98	0.606	176.58
7 3	PLA	330	325	27.37	0.688	26.95	0.716	141.56
8 2	PLA	205	171	17	0.2	14.18	0.236	246.61
10 2	PLA	449	396	37.24	0.478	32.84	0.866	233.79
10 3	PLA	410	332	34	0.541	27.53	0.708	335.36

Source: Own elaboration.

The ABS and PLA exhibit a strong positive correlation between their tensile mechanical properties and the parameters TBT and ID. ABS displays a strong positive correlation with ILD1 and a weak negative correlation with TBLD1. In contrast, PLA demonstrates a weak positive correlation with ILD1 and a strong negative correlation with PS. Furthermore, PLA reveals a strong negative correlation for certain mechanical properties with PS and a weak negative correlation with WST.

Visual Explorative data analysis

FreeViz is used to analyze relations between factors and the Young's Module response, and compare with correlation results. Visual tools are show in Figures 6 and 7. The trend of the positive and negative factors is the same as in Table 5 and 6, with INFILLDENSITY, TOPBOTTOMTHICKNESS in direct strong correlation with the response.

Table 5. Correlation matrix for ABS material ABS

	MAX LOAD (N)	MAX STRESS (MPa)	BREAK STRESS (Mpa)	E(MPa)
LH	-0.071	-0.062	-0.147	-0.051
WT	0.329	0.320	0.283	0.086
TBT	0.531	0.548	0.461	0.396
TBLD1	-0.345	-0.330	-0.324	-0.334
TBLD2	0.198	0.177	0.151	0.357
ID	0.736	0.719	0.730	0.834
ILD1	0.545	0.540	0.547	0.536
ILD2	0.180	0.165	0.181	0.219
WST	-0.275	-0.299	-0.239	-0.062
ET	0.318	0.309	0.290	0.187
BT	-0.063	-0.043	-0.040	-0.218
PS	-0.209	-0.233	-0.128	-0.079

Source: Own elaboration.

Table 6. Correlation matrix for PLA material

	MAX LOAD (N)	MAX STRESS (MPa)	BREAK STRESS (Mpa)	E(MPa)
LH	0.255	0.255	0.007	0.119
WT	0.097	0.097	0.181	0.036
TBT	0.640	0.640	0.439	0.290
TBLD1	-0.041	-0.041	0.011	0.261
TBLD2	0.286	0.286	0.122	0.312
ID	0.472	0.472	0.259	0.466
ILD1	0.343	0.343	0.277	0.139
ILD2	-0.147	-0.147	-0.113	-0.102
WST	-0.344	-0.344	-0.321	0.128
ET	-0.200	-0.200	-0.068	-0.180
BT	0.087	0.087	0.069	-0.061
PS	-0.529	-0.529	-0.389	-0.242

Source: Own elaboration.

Figure 6. FreeViz for ABS

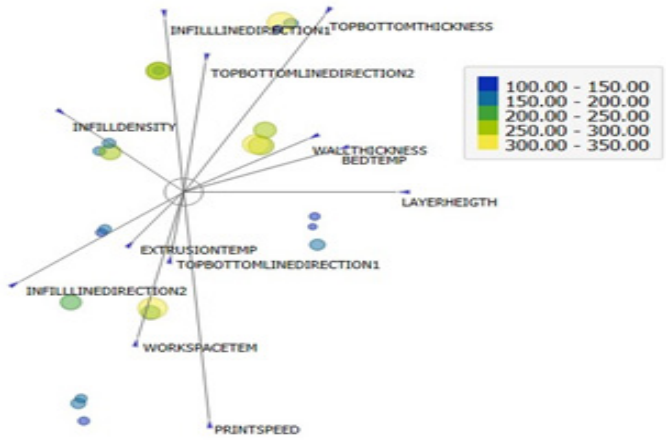

Source: Own elaboration.

Figure 7. FreeViz for PLA

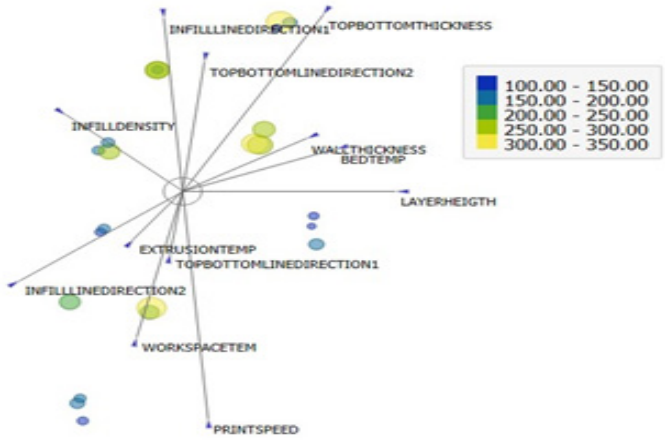

Source: Own elaboration.

Violin and Box plots for Printing positions

Most of the ML algorithms work with numerical factors or categorical factors with only two levels. Position factor has three levels, in this case violin and box plot are used for the visual comparison of the results in Figure 8.

Figure 8. Violin plot for POS Vs. Young's Module and PLA - ABS.

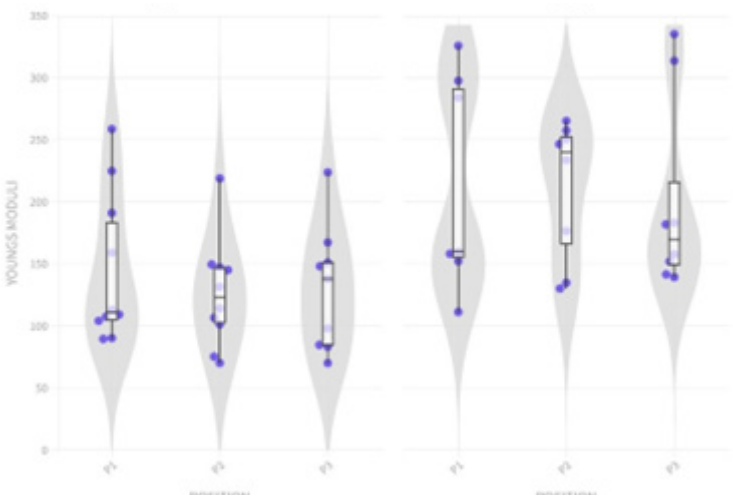

Source: Own elaboration.

In comparing the two materials with respect to the modulus of elasticity, the results indicate that, on average, PLA exhibits a higher mean response, and that Position 2 is most favorable for achieving a higher modulus of elasticity. Conversely, for ABS, Position 3 is found to be more suitable for obtaining a greater mean response in the modulus of elasticity.

Figure 9 shows the comparative between position and materials for Beak stress response. The comparison reveals that for break stress, PLA exhibits higher average values at Position 1, while ABS shows lower average values compared to PLA, with its highest mean value occurring at Position 1.

Figure 9. Violin plot for POS Vs. Break stress and PLA – ABS.

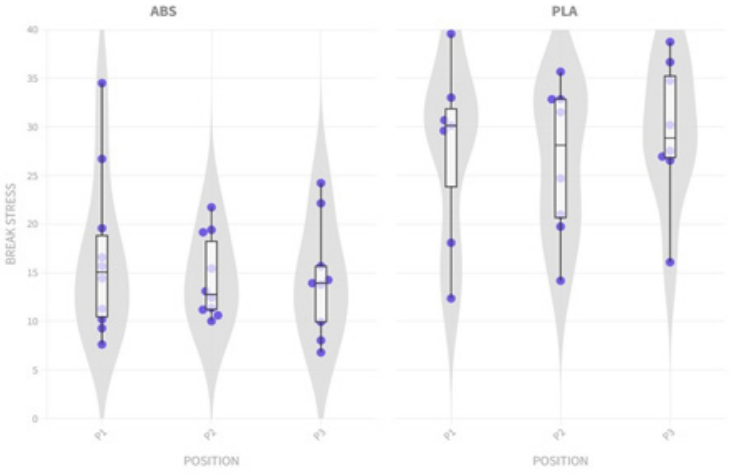

Source: Own elaboration.

Figure 10 shows the comparative between position and materials for maximum stress response. In the comparative analysis of position, material, and maximum stress, it can be inferred from the results that PLA exhibits higher average maximum stress values compared to ABS. The most favorable position for PLA is Position 3, whereas for ABS, the highest average value is observed at Position 1.

Figure 10. Violin plot for POS Vs. maximum stress and PLA – ABS

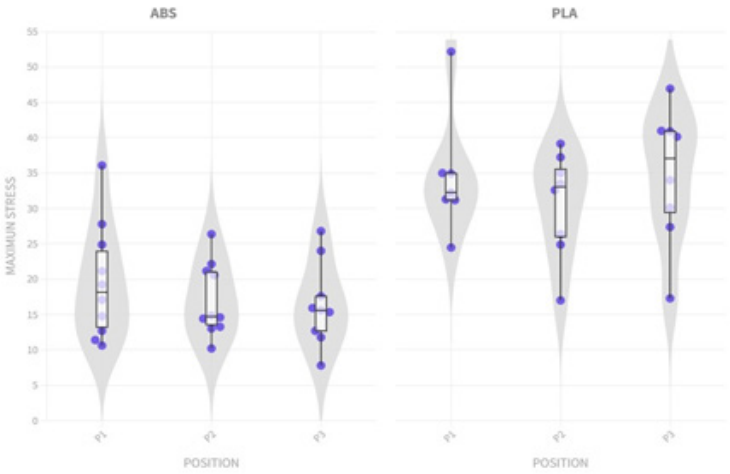

Source: Own elaboration.

Conclussions

Fourteen parameters were analyzed using machine learning techniques for a 3D printing process for ABS and PLA printing materials. Significant correlation were identified, with strong and weak relations between parameters and mechanical strength response for tensile test.

It was found that TBT and ID increase the tensile strength response for both materials. PLA demonstrates a strong negative correlation with PS.

Position 1 and 3 are better to obtain maximum average responses in mechanical tension properties.

For future works, research on the deposited line directions in the infill and top-bottom with different infill patterns shall be considered for both materials, and research about different infill patterns too.

References

1. S. Vyavahare, S. Teraiya, D. Panghal, and S. Kumar, 'Fused deposition modelling: a review', Rapid Prototyping Journal, vol. 26, pp. 176–201, 2020. DOI: 10.1108/rpj-04-2019-0106
2. G. Gao, F. Xu, J. Xu, G. Tang, and Z. Liu, "A Survey of the Influence of Process Parameters on Mechanical Properties of Fused Deposition Modeling Parts," Micromachines, vol. 13, no. 4, p. 553, Mar. 2022. DOI: 10.3390/mi13040553.
3. A. Dey and N. Yodo, "A Systematic Survey of FDM Process Parameter Optimization and Their Influence on Part Characteristics," Journal of Manufacturing and Materials Processing, vol. 3, no. 3, p. 64, Jul. 2019. DOI: 10.3390/jmmp3030064.
4. I. A. Rosid and A. E. Tontowi, 'Parameter optimization of customized fdm 3d printer machine for biocomposite material [sago/pmma] using 2k fractional factorial design', OPSI, vol. 14, no. 2, pp. 188–196, 2021. DOI: https://doi.org/10.31315/opsi.v14i2.5352
5. A. H. M. Haidiezul, M. H. M. Hazwan, W. S. Lee, Gunalan, N. F. Najihah, and I. Fadhli, 'Shrinkage optimisation on the 3D printed part using Full Factorial Design (FFD) optimisation approach', IOP Conference Series: Materials Science and Engineering, vol. 932, no. 1, p. 012109, Sep. 2020. DOI 10.1088/1757-899X/932/1/012109
6. E. R. Bialete et al., 'Characterization of the Tensile Strength of FDM-Printed Parts Made from Polylactic Acid Filament using 33 Full-Factorial Design of Experiment', in 2020 IEEE 12th International Conference on Humanoid, Nanotechnology, Information Technology, Communication and Control, Environment, and Management (HNICEM), 2020, pp. 1–6. DOI: 10.1109/HNICEM51456.2020.9400089
7. P. Rodríguez, P. Zapico, P. E. Robles, A. Soto, and J. Barreiro, 'Evaluation of mechanical properties of FDM components reinforced with fibre', IOP Conference Series: Materials Science and Engineering, vol. 1193, no. 1, p. 012069, Oct. 2021. DOI 10.1088/1757-899X/1193/1/012069
8. S. Pawar and D. Dolas, 'Effect of process parameters on flexural strength and surface roughness in fused deposition modeling of PC-ABS material', Journal of Micromanufacturing, vol. 5, no. 2, pp. 164–170, 2022. https://doi.org/10.1177/25165984211031
9. T. Nancharaiah, 'Optimization of Process Parameters in FDM Process Using Design of Experiments', 2011.
10. R. Srinivasan, T. Pridhar, L. S. Ramprasath, N. S. Charan, and W. Ruban, 'Prediction of tensile strength in FDM printed ABS parts using response surface methodology (RSM)', Materials Today: Proceedings, vol. 27, pp. 1827–1832, 2020. https://doi.org/10.1016/j.matpr.2020.03.788
11. G. Gao, F. Xu, and J. Xu, "Parametric Optimization of FDM Process for Improving Mechanical Strengths Using Taguchi Method and Response Surface Method: A Comparative Investigation," Machines, vol. 10, no. 9, p. 750, Aug. 2022, doi: 10.3390/machines10090750.
12. O. A. Mohamed, S. H. Masood, and J. L. Bhowmik, 'Mathematical modeling and FDM process parameters optimization using response surface methodology based on Q-optimal design', Applied Mathematical Modelling, vol. 40, no. 23, pp. 10052–10073, 2016. https://doi.org/10.1016/j.apm.2016.06.055
13. M. Waseem et al., "Multi-Response Optimization of Tensile Creep Behavior of PLA 3D Printed Parts Using Categorical Response Surface Methodology," Polymers, vol. 12, no. 12, p. 2962, Dec. 2020, doi: 10.3390/polym12122962.
14. M. Vorkapić, I. Mladenović, M. Pergal, T. Ivanov, and M. Baltić, 'Optimisation of tensile stress of poly (lactic acid) 3D printed materials using response surface methodology', Tribology and Materials, vol. 1, no. 2, pp. 70–80, 2022. https://doi.org/10.46793/tribomat.2022.009
15. M. Hikmat, S. Rostam, and Y. M. Ahmed, 'Investigation of tensile property-based Taguchi method of PLA parts fabricated by FDM 3D printing technology', Results in Engineering, vol. 11, p. 100264, 2021. https://doi.org/10.1016/j.rineng.2021.100264
16. M. Kam, A. İpekçi, and Ö. Şengül, 'Investigation of the effect of FDM process parameters on mechanical properties of 3D printed PA12 samples using Taguchi method', Journal of Thermoplastic Composite Materials, vol. 36, no. 1, pp. 307–325, 2023. https://doi.org/10.1177/089270572110064

17. N. Maguluri, G. Suresh, and K. V. Rao, 'Assessing the effect of FDM processing parameters on mechanical properties of PLA parts using Taguchi method', Journal of Thermoplastic Composite Materials, vol. 36, no. 4, pp. 1472–1488, 2023. https://doi.org/10.1177/08927057211053
18. K. Sharma, K. Kumar, K. R. Singh, and M. S. Rawat, 'Optimization of FDM 3D printing process parameters using Taguchi technique', IOP Conference Series: Materials Science and Engineering, vol. 1168, no. 1, p. 012022, Jul. 2021. DOI 10.1088/1757-899X/1168/1/012022
19. M. Abouelmajd et al., 'Experimental analysis and optimization of mechanical properties of FDM-processed polylactic acid using Taguchi design of experiment', International Journal for Simulation and Multidisciplinary Design Optimization, vol. 12, p. 30, 2021. https://doi.org/10.1051/smdo/2021031
20. G. D. Goh, S. L. Sing, and W. Y. Yeong, 'A review on machine learning in 3D printing: applications, potential, and challenges', Artificial Intelligence Review, vol. 54, no. 1, pp. 63–94, 2021. https://doi.org/10.1007/s10462-020-09876-9
21. N. S. Johnson et al., 'Machine Learning for Materials Developments in Metals Additive Manufacturing', arXiv preprint arXiv:2005. 05235, 2020. https://doi.org/10.48550/arXiv.2005.05235
22. T. Sarkar, 'doepy', GitHub repository. GitHub. Available: https://github.com/tirthajyoti/doepy
23. ASTM International, ASTM D638-14, Standard Test Method for Tensile Properties of Plastics. ASTM International, 2015. DOI: 10.1520/D0638-14
24. U. of L. Bioinformatics Laboratory, "Data Mining," Orange Data Mining - Data Mining, https://orangedatamining.com/ (accessed Oct. 24, 2023).
25. U. of L. Bioinformatics Laboratory, "oRANGE Correlations," Orange Data Mining - Data Mining, https://orangedatamining.com/widget-catalog/unsupervised/correlations/ (accessed Oct. 24, 2023).